

Hydrogenation of Glucose on a Carbon-Supported Ru Catalyst: Optimization of the Reaction Conditions

Juan J. Musci^{1,2}, María E. Chiosso^{1,2}, Guillermo J. Siri³, Mónica L. Casella^{1,3}

¹Departamento de Ciencias Básicas y Experimentales, Universidad Nacional del Noroeste de la Provincia de Buenos Aires, Junín, Argentina

²Centro de Investigaciones y Transferencia del Noroeste de la Provincia de Buenos Aires (CITNOBA) - UNNOBA-UNSAaA-CONICET, Pergamino, Argentina

³Centro de Investigación y Desarrollo en Ciencias Aplicadas “Dr. Jorge J. Ronco” (CINDECA) CCT CONICET-La Plata, Universidad Nacional de La Plata, Comisión de Investigaciones Científicas, La Plata, Argentina

Email: jjmusci@comunidad.unnoba.edu.ar

How to cite this paper: Musci, J.J., Chiosso, M.E., Siri, G.J. and Casella, M.L. (2023) Hydrogenation of Glucose on a Carbon-Supported Ru Catalyst: Optimization of the Reaction Conditions. *Advances in Chemical Engineering and Science*, 13, 224-240. <https://doi.org/10.4236/aces.2023.133016>

Received: March 28, 2023

Accepted: June 12, 2023

Published: June 15, 2023

Copyright © 2023 by author(s) and Scientific Research Publishing Inc. This work is licensed under the Creative Commons Attribution International License (CC BY 4.0).

<http://creativecommons.org/licenses/by/4.0/>



Open Access

Abstract

The catalytic hydrogenation of D-glucose over a 3 wt% Ru/C catalyst was studied varying the operating conditions in mild conditions range to optimize the obtention of D-sorbitol. The stirring speed, temperature, pressure, and initial glucose concentration were varied between 250 - 700 rpm, 343 - 383 K, 0.5 - 2 MPa, and 0.033 - 0.133 M, respectively. To verify the absence of mass transport limitations, the diffusion of reagents in the gas-liquid interface, the liquid-solid interface, and the internal diffusion in the particles were evaluated. Under the operating conditions studied, the reaction rate showed an order with respect to H₂ of 0.586 and with respect to glucose of 0.406. The kinetic data were adjusted using 3 general models and 19 different sub-models based on Langmuir-Hinshelwood-Hougen-Watson (LHHW) kinetics. Model 3a was the best one interpreting the aqueous phase hydrogenation of glucose (both reagents competitively adsorbed on the catalyst). The H₂ adsorption is dissociative and the rate-limiting step is the surface chemical reaction.

Keywords

3 wt% Ru/C, D-Glucose, Hydrogenation, Kinetic Modeling

1. Introduction

The use of renewable raw materials and the development of different strategies

for the valorization of biomass, together with heterogeneous catalysis, are interesting alternatives for the substitution of fossil fuel resources in order to obtain intermediates and final chemical products of high added value [1]. Cellulose is the most abundant carbohydrate and it is inedible. For this reason, it is expected to be the first objective of the chemistry of biomass resources [2]. By degrading cellulosic biomass, mono-, di- and oligosaccharides can be obtained, which in turn can be transformed into valuable final chemical products or intermediates [3]. Among the most important chemical products derived from cellulosic biomass are sugar alcohols.

In 2004, the US Department of Energy [4] identified D-sorbitol as one of the 12 most important value-added chemicals that can be obtained from biomass. D-sorbitol is a potential source of alkanes for liquid biofuels [5]. Esters and other derivatives of D-sorbitol are also important additives and intermediates in the cosmetics and pharmaceutical industries, with the molecule being a key substitute for sugar in the food and beverage industry [6].

Sorbitol is the main product of glucose hydrogenation [4]. However, while hydrogenation of D-glucose to D-sorbitol seems like a simple reaction, D-glucose is not only selectively converted to D-sorbitol, but it can also give many other byproducts (see Figure 1). Some of these by-products can even cause catalyst deactivation [7]. Sorbitol, like other hexitols, can also form chelate complexes with nickel (or Cu, Fe) readily in an aqueous solution. These complexes are stable under alkaline conditions, which results in nickel being left in the sorbitol solution. [8] [9] [10].

Among the possible competitive reactions, the Lobry rearrangement of Bruyn-Alberda van Ekenstein of D-glucose results in the formation of D-mannose and D-fructose. Aldehydes (glyceraldehyde, formaldehyde) and

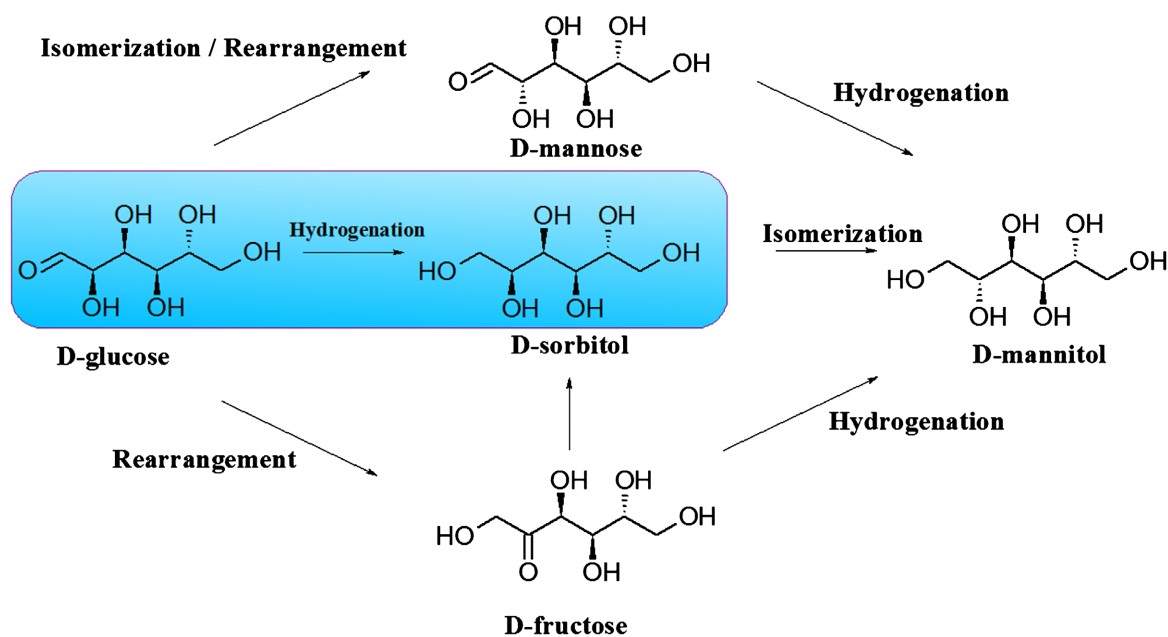


Figure 1. Reaction network of the hydrogenation of d-glucose.

ketones (dihydroxyacetone) could originate by cleavage in an alkaline medium of sugar molecules. This reaction occurs via an enediol intermediate via a proton-transfer mechanism [11]. The hydrogenation in the liquid phase of D-glucose generally leads as a main product to D-sorbitol but alkaline conditions could favor both the procedures of glucose isomerization and sorbitol hydrogenolysis, giving mannitol as main by-product and lower alcohols such as propanediol and ethylene glycol [12]. On the other hand, under acidic conditions, 5-hydroxymethylfurfural and levulinic acid can be formed by dehydration of glucose [13]. The way to adjust the selectivity to the desired product is through a correct selection of the active metal, the catalytic support, and the reaction conditions such as temperature and hydrogen pressure.

Historically, glucose has been hydrogenated to sorbitol over Ni catalysts. One of the advantages of the use of a Ni catalyst is its relatively low price compared to other more expensive catalytic systems. However, Ni presents the problem of leaching and as a consequence, purification of the obtained sorbitol is necessary [14]. It has been found that ruthenium-based catalysts outperform nickel-based catalysts due to their high activity, lower load requirement, and lower deactivation [8] [14] [15] [16]. Clearly, the price of metallic ruthenium as a raw material is much higher than that of nickel. However, other issues must be taken into account when comparing the final cost of each catalyst. Thus, the metallic load of the catalysts and the possibility of their reuse must be analyzed. Thus, although it is more expensive than nickel, it may be of interest for industrial uses.

The kinetics of glucose hydrogenation over different Ru catalysts varying reaction conditions have been recently reviewed by Ahmed and Hameed [17]. The authors described published results of kinetic data and the effect of the initial concentration of glucose, temperature and pressure on the rate constants and the selectivity to sorbitol. However, most of these results were obtained at high values of pressure and temperature.

As a contribution, in this work, the aqueous phase hydrogenation (APH) of glucose on a 3 wt% Ru/C catalyst is studied, establishing mild conditions of temperature, pressure, and agitation which are lower than the ones generally reported and optimize the obtention of the desired product. Kinetic modeling was developed using models based on Langmuir-Hinshelwood-Hougen-Watson (LHHW) kinetics.

2. Experimental

2.1. Catalyst Preparation and Characterization

A Ru catalyst, with a metal loading of 3 wt%, was prepared by impregnation with excess solution on a commercial activated carbon (C) (NORIT, ground, and sieved to 60 - 100 mesh) according to reference [18].

Textural properties of the support, pore volume (V_p), and specific surface area (S_{BET}) were established by N_2 physisorption at 77 K using a *Micromeritics ASAP 2020* equipment.

The size distribution of metallic particles was determined by transmission electron microscopy (TEM) with a JEOL 100 CX II microscope. The mean particle size (d_{TEM}) was calculated using Equation (1):

$$d_{\text{TEM}} = \frac{\sum_i n_i d_i^3}{\sum_i n_i d_i^2} \quad (1)$$

where d_i is the diameter of particle and n_i is the number of particles with size d_i .

The reducibility of the catalyst was studied by Temperature-Programmed Reduction (TPR) experiments using a laboratory-constructed equipment and X-ray photoelectron spectroscopy (XPS) analysis were performed on a Specs Multi-technique system (SPECS) equipped with a dual Mg/Al X-ray source and a PHOIBOS 150 hemispherical analyzer operating in the Fixed Analyzer Transmission (FAT) mode. Both characterizations were conducted following previously published protocols [18].

2.2. Catalytic Tests

The tests were carried out in a high-pressure reactor, using 0.25 g of catalyst and 50 mL of water as solvent. The reaction time was 7 h. The stirring speed, the temperature, the pressure, and the initial glucose concentration were varied between 250 - 700 rpm, 343 - 383 K, 0.5 - 2 MPa, and 0.033 - 0.133 M, respectively. The variables were modified one at a time, keeping the others constant in each test.

The reaction samples were analyzed offline by liquid chromatography in a UHPLC chromatograph equipped with a RI-detector (operating at 313 K). Separation of the components was achieved by a Phenomenex Rezex RCM Ca^{+2} Monosaccharide (300 × 7.8 mm) column operated at 353 K. Elution was performed at 0.6 mL/min flow rate of mobile phase (milli-Q-water).

The conversion of glucose (Glu) was calculated using the following expression:

$$x(\%)_{\text{Glu}} = \frac{C_{\text{Glu}}^0 - C_{\text{Glu}}^t}{C_{\text{Glu}}^0} \cdot 100 \quad (2)$$

Analytical criteria were verified to determine the absence of diffusional limitations and the experimental results were interpreted by kinetic modeling using heterogeneous models of Langmuir-Hinshelwood-Hougen-Watson (LHHW).

3. Results and Discussion

3.1. Catalyst Characterization

The activated carbon used as support had a pore volume of 0.53 $\text{cm}^3 \cdot \text{g}^{-1}$ and a S_{BET} of 1000 $\text{m}^2 \cdot \text{g}^{-1}$ measured by N_2 physisorption. The 3 wt% Ru/C catalyst has been deeply characterized, as previously published [18]. In order to better explain the kinetic results, the main characteristics of the catalyst are gathered in **Table 1**.

Briefly, it can be said that TEM analysis showed the presence of small and

Table 1. Ru 3 wt%/C catalyst preparation and characterization.

Property	Value
Support Surface Area and Pore Volume	1000 m ² ·g ⁻¹ and 0.53 cm ³ ·g ⁻¹
Ru Particle Diameter (measured by TEM)	1.1 nm
Ru Dispersion (based on TEM results) ^a	81%
H ₂ Consumption (TPR)	413 K (decomposition of the functional groups of the support surface)
	463 K (reduction of Ru(III) to Ru(0))
	523 K (gasification of surface carbon atoms located around the metal particles)
Ru oxidation state (XPS)	BE of Ru 3d _{5/2} : 280.5 eV (metallic form)

a. $D_{Ru} = \frac{0.91}{d_{TEM}}$ [19].

uniform-sized particles that are widely dispersed, and Ru is in the metallic form as was confirmed by XPS and TPR analysis.

3.2. Mass Transfer Limitation

Analytical criteria were used to compare the initial reaction rate with the maximum transport rates in the physical stages. In the case of liquid-phase hydrogenation reactions, the diffusion of reagents and/or products in the gas-liquid interface, the liquid-solid interface, and internal diffusion in the particles must be evaluated.

The reaction conditions used to determine the initial reaction rate were 363 K, 1.25 MPa of H₂ pressure, and a stirring speed of 625 rpm, using 0.25 g of 3 wt% Ru/C catalyst and 0.90 g of glucose as substrate. From the conversion vs. time curve, the initial reaction rate was calculated at 10% conversion.

3.2.1. Gas-Liquid Mass Transfer Limitations

To ensure that there is no resistance to H₂ transport at the gas-liquid interface, the criterion determined by the ratio between the observed reaction rate and the maximum transfer rate based on the liquid volume (α_1) was used.

$$\alpha_1 = \frac{(r_i)_{obs}}{k_L \cdot a_G \cdot C_{H_2}} \leq 0.1 \quad (3)$$

The criterion states that, if the reaction rate observed is less than 10% of the maximum gas-liquid mass transfer rate, then the transport process is much faster than the observed chemical reaction, thus not limiting the overall process.

For the calculation of the $k_L \cdot a_G$ coefficient several correlations determined by different authors can be used. One of them is the proposed by Meille *et al.* [20] who studied the determination of the $k_L \cdot a_G$ coefficient in laboratory tank reactors, with magnetic stirring and without the use of baffles, with volumes between 25 and 300 cm³ (systems with similar properties to those used in this

work). Considering a reactor of 150 cm³ of capacity, which is the most similar to the one used in this work, the correlation is:

$$k_l \cdot a_G = 1.14 \times 10^{-4} \cdot N^{2.98} \quad (4)$$

The results gathered in **Table 2** show that under the conditions employed in the present work, there are no limitations for the H₂ transport at the gas-liquid interface and within the reaction volume.

3.2.2. Liquid-Solid Mass Transfer Limitations

In order to determine the absence of mass transfer limitations of the reagents in the liquid-solid interface, the selected criterion is similar to that seen for the gas-liquid interface. In this case (α_2) for both reagents (H₂ and glucose), the ratio between the reaction rate and the mass transport rate must be less than 10% (Equation (5)).

$$\alpha_2 = \frac{(r_i)_{obs}}{k_C \cdot a_C \cdot m_c \cdot C_i} \leq 0.1 \quad (5)$$

As can be seen in **Table 2**, the criterion is satisfactorily fulfilled for the conditions tested, for both glucose and H₂.

3.2.3. Internal Diffusion Limitation

To verify if there is resistance to mass transfer inside the catalyst particles, the Weisz-Prater criterion was used [21] [22] for both reactants (H₂ and glucose). According to this criterion, the mass transfer limitations are negligible if it is satisfied that:

$$\Phi = \frac{(r_i)_{obs} \cdot L^2}{D_i^e \cdot C_i^S} \ll 1 \quad (6)$$

For both H₂ and glucose, the Weisz-Prater criterion is fulfilled, since for both reactants the value of Φ is much smaller than 1 (see **Table 2**). Thus, it can be said that there are no limitations to the intraparticle mass transfer.

3.3. Influence of Stirring Speed

Agitation of the reaction mixture in a slurry reactor is important not only to keep the catalyst particles uniformly suspended, but also to facilitate the transport of the gaseous reactant through the gas-liquid interface and the dissolved reagent in the liquid medium towards the surface of the catalyst, there being a

Table 2. Parameters and correlations used in the verification of transport limitation.

Initial rate observed $(r_i)_{obs}$ [mol/L.s]	External mass transport Gas-liquid interface $\alpha_1 = \frac{(r_i)_{obs}}{k_L \cdot a_G \cdot C_{H_2}} \leq 0.1$	External mass transport Liquid-solid interface $\alpha_2 = \frac{(r_i)_{obs}}{k_C \cdot a_C \cdot m_c \cdot C_i} \leq 0.1$		Internal mass transport $\Phi = \frac{(r_i)_{obs} \cdot L^2}{D_i^e \cdot C_i^S} \ll 1$		
Parameter	α_1	α_{2-H_2}	α_{2-glu}	Φ_{H_2}	Φ_{glu}	
Value	6.6×10^{-6}	5.17×10^{-3}	0.10	0.04	0.097	0.087

relation between the increase of the stirring speed and the increase of the mass transfer coefficient.

In order to ensure the absence of mass transfer limitations in the gas-liquid interface, experiments were carried out varying the stirring speed between 250 and 700 rpm at 363 K and 1.25 MPa of H₂ pressure, with 0.25 g of Ru/C catalyst and 0.90 g of glucose as substrate. **Figure 2** shows the initial reaction rates (r_i) for each stirring speed, calculated from the slopes of the conversion vs. time curves (at 10% conversion). With stirring speeds lower than approximately 600 rpm, (r_i) decreases, indicating the presence of limitations to the transfer of hydrogen at the gas-liquid interface. For this reason, a speed of 625 rpm was adopted for subsequent tests.

3.4. Influence of Reaction Parameters

The influence of temperature on the catalytic activity at 1.25 MPa H₂ and 0.1 M of glucose was investigated (**Figure 3**), varying its value from 343 K to 383 K.

Below 353 K, the reaction rate decreases significantly, and only 80% glucose conversion is reached at 343 K after 7 h of reaction. Above 373 K, it is observed that the time necessary to achieve complete conversion is reduced to 5 h. However,

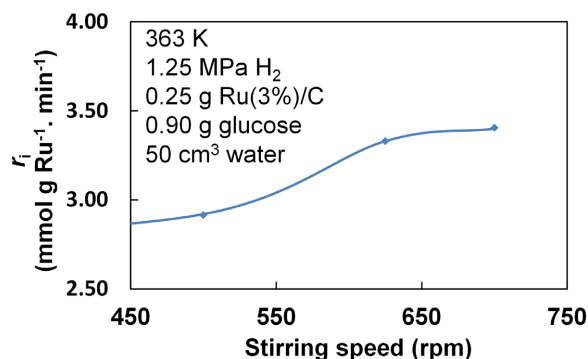


Figure 2. Effect of the stirring speed on the initial D-glucose hydrogenation rate. [$T = 363$ K , $p_{\text{H}_2} = 1.25$ MPa , $W_{\text{CAT}} = 250$ mg , $C_{\text{glu}}^0 = 0.1$ M ; $V_{\text{H}_2\text{O}} = 50$ ml].

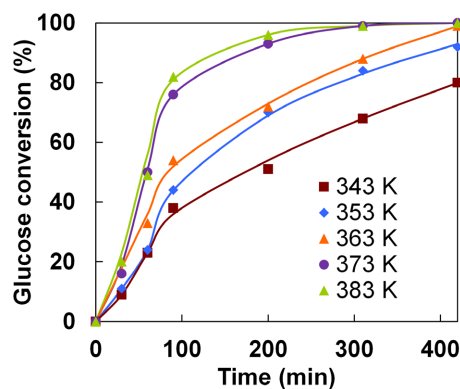


Figure 3. Effect of temperature on glucose APH with Ru (3%)/C. In symbols, experimental results and solid lines the results using the best model (3a). [$p_{\text{H}_2} = 1.25$ MPa , $W_{\text{CAT}} = 250$ mg , $C_{\text{glu}}^0 = 0.1$ M ; $V_{\text{H}_2\text{O}} = 50$ ml].

in the total time studied (7 h), at 363 K, 99% conversion is achieved. Thus, although time is longer, high conversion is achieved in milder condition. In all the cases, the selectivity was 100% to sorbitol, proving that consecutive or parallel reactions such as isomerizations do not occur (see **Figure 1**).

The apparent activation energy (E_a) was determined by linear regression using an Arrhenius type function. A value of 30.8 kJ/mol was obtained. This value is similar to those reported in literature [17]. Thus, kinetic data using different ruthenium catalysts and various experimental conditions have been reported. In this sense, an activation energy of 32.9 kJ/mol and first-order kinetics with respect to glucose concentration has been reported by Mishra *et al.* [23] over Ru/HY zeolite. Crezee *et al.* [24] reported an activation energy of 55 kJ/mol at 4 MPa of H_2 and 0.75 g/L of 5% Ru/C. Similar values have also been reported in studies carried out with other monosaccharides. Li *et al.* [25] reported that the apparent activation energy (E_a) of maltose hydrogenation using a Ru-P catalyst was 27 kJ/mol (6.45 kcal/mol) and for Ru-B was 32 kJ/mol (7.65 kcal/mol), using a maltose solution of 40% w/v, 363 K, 2 MPa pressure and stirring at 1200 rpm.

The effect of partial pressure of hydrogen (at 363 K and 0.1 M glucose) is presented in **Figure 4**.

It is observed that in every case an almost total conversion was obtained, increasing r_i with the increase of pressure. The variation of the pressure does not produce changes in the selectivity, obtaining sorbitol as the only product.

The reaction order with respect to hydrogen was calculated by considering for r_i a power law rate equation:

$$r_i = k \cdot (C_{\text{glu}})^n \cdot (P_{H_2})^m \quad (7)$$

The linear regression of data obtained shows a reaction order with respect to the H_2 of 0.586. This value was in reasonable agreement with that reported by Zhang *et al.* of 0.66 over silica-supported Pt nanoparticles [6] and also with that informed by Tukac of 0.65 [26]. This latter value was obtained in the catalytic hydrogenation of glucose, using a 40 wt% aqueous solution of D-glucose and a

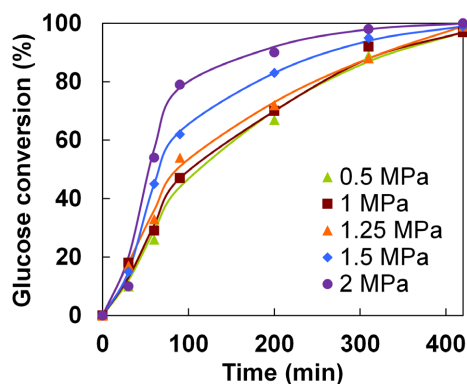


Figure 4. Effect of H_2 pressure on glucose APH with Ru (3%)/C. In symbols, experimental results and in solid lines the results using the best model (3a). [$T = 363$ K ,

$W_{\text{CAT}} = 250$ mg , $C_{\text{glu}}^0 = 0.1$ M ; $V_{H_2O} = 50$ ml].

kieselgur-supported nickel catalysts (12% NiO, 2% Cr₂O₃). The temperature range was 388 to 433 K and pressure range of 0.5 - 10 MPa [19].

The results of the variation of the initial glucose concentration (at 363 K and 1.25 MPa) are given in **Figure 5**.

Although the final conversion reached after 7 h of reaction decreases, the activity of the catalyst increases with increasing glucose concentration. The reaction order with respect to glucose was determined by linear regression from the data with Equation (8) and a value of 0.406 was obtained. In the literature, it has been reported that glucose concentration presents a relatively complex influence upon the hydrogenation rate. Guo *et al.* [27] studying a Ru-B amorphous catalyst, observed that increasing glucose concentration the initial rate increased linearly up to 40 wt% and then presented a plateau at higher glucose concentration. This kinetic behavior could be explained by the adsorption strength of glucose and hydrogen on the catalyst. The glucose molecule adsorbs strongly on the catalyst reaching saturated adsorption even at low concentration. Only when the glucose concentration was very low in the liquid phase, and in consequence, the surface adsorption was unsaturated, the hydrogenation rate grew up with the glucose concentration.

The catalytic hydrogenation of D-glucose is generally described by means of Langmuir-Hinshelwood kinetics with a change from first-order dependency in D-glucose at low concentrations to zero-order behavior at high concentrations [8].

3.5. Kinetic Modeling

Based on the above-discussed results, the following hypotheses for the formulation of the LHHW models were considered:

1) The superficial hydrogenation reaction is irreversible (total conversion of glucose to sorbitol was obtained in the experiments performed).

2) Hydrogen concentration in the liquid phase is constant, due to the constant pressure of hydrogen throughout the test, the high volume of solvent and the

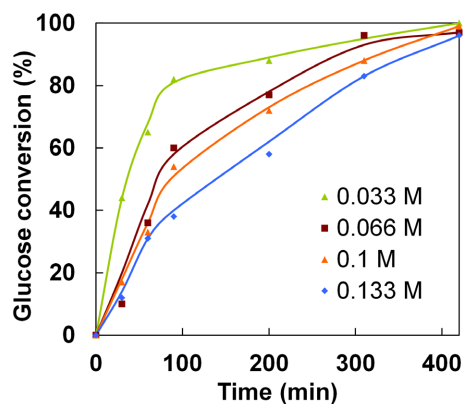


Figure 5. Effect of initial glucose concentration on glucose APH with Ru (3%)/C. In symbols, experimental results and in solid lines the results using the best model (3a) [$p_{\text{H}_2} = 1.25$ MPa , $T = 363$ K , $W_{\text{CAT}} = 250$ mg , $V_{\text{H}_2\text{O}} = 50$ ml].

efficient mixing.

Three general models were proposed: a first model of the Eley-Rideal type, with only glucose adsorption on the solid catalyst; a second model with adsorption of molecular hydrogen in addition to glucose adsorption and a third model considering the dissociative adsorption of hydrogen. Both models, 2 and 3, considered the competitive adsorption of H₂ and glucose. By assuming different rate limiting steps (r.l.s.), (H₂ adsorption, glucose adsorption or surface chemical reaction) and the possibility or not of sorbitol (the reaction product) adsorption, 19 different LHHW sub models were analyzed.

The equations were solved numerically using the algorithm of Runge-Kutta-Merson with the data obtained at 363 K. The estimation of model parameters was performed by non-linear regression, using a Levenberg-Marquardt algorithm that minimizes the objective function:

$$S = \sum_{i=1}^n (C_{i,t}^* - C_{i,t}^{\text{CALC}})^2 \quad (8)$$

Table 3 presents the proposed LHHW models, with the estimated parameters

Table 3. Overview of model equations and kinetic modeling results using LHHW models.

Model equation/Mechanism	Parameter estimation	<i>r</i>	MSC
$r = \frac{k_d K_A [C_A^{g0} (1-X) C_B^{g0}]}{1 + K_A C_A^{g0} (1-X) + K_C (C_C^{g0} + C_A^{g0} X)}$ 1a. Glucose adsorption. r.l.s.: surface reaction.	$k_d = 2.10$ $K_A = 3.32 \times 10^7$ $K_C = 4.10 \times 10^7$	0.951	2.264
$r = \frac{k_d K_A [C_A^{g0} (1-X) C_B^{g0}]}{1 + K_A C_A^{g0} (1-X)}$ 1b. Glucose adsorption. There is no sorbitol adsorption. r.l.s.: surface reaction.	$k_d = 1.02$ $K_A = 5.84 \times 10^2$	0.907	1.523
$r_{anA} = \frac{k_{aA} (C_A^{g0} (1-X))}{1 + K_C (C_C^{g0} + C_A^{g0} X)}$ 1c. Glucose adsorption. r.l.s.: glucose adsorption.	$k_{aA} = 5.60 \times 10^{-1}$ $K_C = 1.54 \times 10^2$	0.926	1.811
$r_{anA} = k_{aA} (C_A^{g0} (1-X))$ 1d. Glucose adsorption. There is no sorbitol adsorption. r.l.s.: glucose adsorption.	$k_{aA} = 7.12 \times 10^{-2}$	0.862	1.615
$r_{anC} = \frac{k_{aC}}{K_C}$ 1e. Glucose adsorption. r.l.s.: sorbitol desorption.	$k_{aC} = 1.78 \times 10^{-2}$ $K_C = 3.22$	0.907	1.297
$r = \frac{k_d K_A K_B (C_A^{g0} (1-X) C_B^{g0})}{[1 + K_A C_A^{g0} (1-X) + K_B C_B^{g0} + K_C (C_C^{g0} + C_A^{g0} X)]^2}$ 2a. Glucose and molecular H ₂ adsorption. r.l.s.: surface reaction.	$k_d = 4.02 \times 10^{-1}$ $K_A = 1.11 \times 10^4$ $K_B = 5.45 \times 10^4$ $K_C = 7.40 \times 10^3$	0.964	2.531
$r = \frac{k_d K_A K_B (C_A^{g0} (1-X) C_B^{g0})}{[1 + K_A C_A^{g0} (1-X) + K_B C_B^{g0}]^2}$ 2b. Glucose and molecular H ₂ adsorption. There is no sorbitol adsorption. r.l.s.: surface reaction.	$k_d = 3.60 \times 10^{-1}$ $K_A = 8.54 \times 10^8$ $K_B = 2.75 \times 10^9$	0.928	1.468

Continued

$r_{anA} = \frac{k_{aA} [C_A^{g0} (1-X)]}{1 + K_B C_B^{g0} + K_C (C_C^{g0} + C_A^{g0} X)}$	$k_{aA} = 1.03 \times 10^{-1}$		
2c. Glucose and molecular H ₂ adsorption. r.l.s.: glucose adsorption.	$K_B = -1.51 \times 10^2$	0.928	1.822
	$K_C = 2.36 \times 10^1$		
$r_{anA} = \frac{k_{aA} [C_A^{g0} (1-X)]}{1 + K_B C_B^{g0}}$	$k_{aA} = 4.32 \times 10^{-2}$	0.870	1.346
2d. Glucose and molecular H ₂ adsorption. There is no sorbitol adsorption. r.l.s.: glucose adsorption.	$K_B = -9.32 \times 10^1$		
$r_{anB} = \frac{k_{aB} C_B^{g0}}{1 + K_A C_A^{g0} (1-X) + K_C (C_C^{g0} + C_A^{g0} X)}$	$k_{aB} = 5.15$		
2e. Glucose and molecular H ₂ adsorption. r.l.s.: H ₂ adsorption.	$K_A = 1.63 \times 10^1$	0.955	2.301
	$K_C = 7.46 \times 10^1$		
$r_{anB} = \frac{k_{aB} C_B^{g0}}{1 + K_A C_A^{g0} (1-X)}$	$k_{aB} = 9.38 \times 10^{-1}$	0.907	1.522
2f. Glucose and molecular H ₂ adsorption. There is no sorbitol adsorption. r.l.s.: H ₂ adsorption.	$K_A = -6.07 \times 10^{-1}$		
$r_{anC} = \frac{k_{aC}}{K_C}$	$k_{aC} = 1.78 \times 10^{-2}$	0.907	1.297
2g. Glucose and molecular H ₂ adsorption. r.l.s.: sorbitol desorption.	$K_C = 3.22$		
$r = \frac{k_d K_A \sqrt{K_B} (C_A^{g0} (1-X) \sqrt{C_B^{g0}})}{(1 + K_A C_A^{g0} (1-X) + \sqrt{K_B C_B^{g0}} + K_C (C_C^{g0} + C_A^{g0} X))^2}$	$k_d = 1.49$		
3a. Glucose and dissociative H ₂ adsorption. r.l.s.: surface reaction.	$K_A = 7.72 \times 10^1$	0.968	2.630
	$K_B = 3.86 \times 10^{-1}$		
	$K_C = 4.75 \times 10^1$		
$r = \frac{k_d K_A \sqrt{K_B} (C_A^{g0} (1-X) \sqrt{C_B^{g0}})}{(1 + K_A C_A^{g0} (1-X) + \sqrt{K_B C_B^{g0}})^2}$	$k_d = -6.80 \times 10^1$		
3b. Glucose and dissociative H ₂ adsorption. There is no sorbitol adsorption. r.l.s.: surface reaction.	$K_A = 2.72 \times 10^1$	0.921	1.638
	$K_B = \sqrt{-3.98 \times 10^{-2}}$		
$r_{anA} = \frac{k_{aA} [C_A^{g0} (1-X)]}{1 + \sqrt{K_B C_B^{g0}} + K_C (C_C^{g0} + C_A^{g0} X)}$	$k_{aA} = 7.65 \times 10^{-2}$		
3c. Glucose and dissociative H ₂ adsorption. r.l.s.: glucose adsorption.	$K_B = \sqrt{-1.23 \times 10^1}$	0.923	1.840
	$K_C = 1.90 \times 10^1$		
$r_{anA} = \frac{k_{aA} [C_A^{g0} (1-X)]}{1 + \sqrt{K_B C_B^{g0}}}$	$k_{aA} = 3.18 \times 10^{-2}$	0.869	1.340
3d. Glucose and dissociative H ₂ adsorption. There is no sorbitol adsorption. r.l.s.: glucose adsorption.	$K_B = \sqrt{-8.62}$		
$r_{anB} = \frac{k_{aB} C_B^{g0}}{(1 + K_A C_A^{g0} (1-X) + K_C (C_C^{g0} + C_A^{g0} X))^2}$	$k_{aB} = 2.94$		
3e. Glucose and dissociative H ₂ adsorption. r.l.s.: H ₂ adsorption.	$K_A = 3.00$	0.948	2.150
	$K_C = 1.15 \times 10^1$		
$r_{anB} = \frac{k_{aB} C_B^{g0}}{(1 + K_A C_A^{g0} (1-X))^2}$	$k_{aB} = 9.36 \times 10^{-1}$	0.907	1.522
3f. Glucose and dissociative H ₂ adsorption. There is no sorbitol adsorption. r.l.s.: H ₂ adsorption.	$K_A = -3.10 \times 10^{-1}$		
$r_{anC} = k_{aC}$	$k_{aC} = 5.53 \times 10^{-3}$	0.907	1.323
3g. Glucose and dissociative H ₂ adsorption. r.l.s.: sorbitol desorption.			

and the correlation coefficients (r). The discrimination between the models was determined, after discarding those with parameters without physical sense, according to the highest r value and using the model selection criterion (MSC), according to the following equation:

$$\text{MSC} = \ln \left(\frac{\sum_{i=1}^n (C_i^* - \bar{C}^*)^2}{\sum_{i=1}^n (C_i^* - C_i^{*\text{CALC}})^2} \right) - \frac{2p}{n_e} \quad (9)$$

The most significant model is the one that leads to the highest MSC value.

Models 2c, 2d, 2f, 3b, 3c, 3d and 3f, have some of their estimated parameters with negative and/or imaginary values, which made them lack of physical sense for the kinetic and equilibrium constants. Because of that, these models are rejected.

In addition, those models that consider that sorbitol is not adsorbed, or that the desorption of this product is the rate limiting step (1b, 1d, 1e, 2b, 2g, 3g) have a poor fit. The adsorption of sorbitol cannot be neglected, however its desorption does not constitute a limitation in the reaction rate ($0 \ll 100$ in the models with the best fit).

The best model among the ones here proposed to interpret the aqueous phase hydrogenation of glucose with 3 wt% Ru/C catalyst (Model 3a) considers that both reagents, glucose and H_2 are adsorbed on the catalyst (competitive adsorption) to give sorbitol, which is then desorbed. The H_2 adsorption is dissociative and the rate limiting step is the surface chemical reaction. Equations (i)-(iv) show the elementary steps describing this process, where (iii) is the r.l.s.:



In **Figure 6**, the experimental results for the conversion of glucose as a function of time with the optimal conditions are presented in symbols, while the values

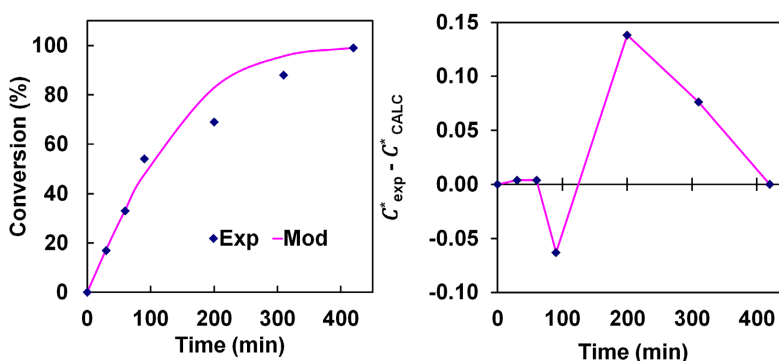


Figure 6. (Left) Aqueous phase hydrogenation (APH) of glucose with Ru (3%)/C in the optimal conditions determined. In symbols, experimental results and in solid lines the results using model 3a. (Right) Evolution of residuals. [$T = 363 \text{ K}$, $p_{\text{H}_2} = 1.25 \text{ MPa}$, $W_{\text{CAT}} = 250 \text{ mg}$, $C_{\text{glu}}^0 = 0.1 \text{ M}$; $V_{\text{H}_2\text{O}} = 50 \text{ ml}$].

estimated by this model are represented in solid lines. As can be seen, a good agreement between the experimental and predicted data is obtained, which validates the kinetic model.

Figure 7 shows the model fit of the other conditions evaluated. Along with this, the distribution of residuals as a function of time is also shown and followed an acceptable random trend, being consistent with the random error hypothesis included in the regression and giving additional support to the adequacy of the model.

Subsequently, the dependence of the kinetic and equilibrium constants with temperature was established using the following expressions:

$$k_d = k_0 e^{\left(\frac{-E_d}{RT}\right)} \quad (10)$$

$$K_A = e^{\left(\frac{-\Delta H_A + \Delta S_A}{RT} + \frac{\Delta S_A}{R}\right)} \quad (11)$$

$$K_B = e^{\left(\frac{-\Delta H_B + \Delta S_B}{RT} + \frac{\Delta S_B}{R}\right)} \quad (12)$$

$$K_C = e^{\left(\frac{-\Delta H_C + \Delta S_C}{RT} + \frac{\Delta S_C}{R}\right)} \quad (13)$$

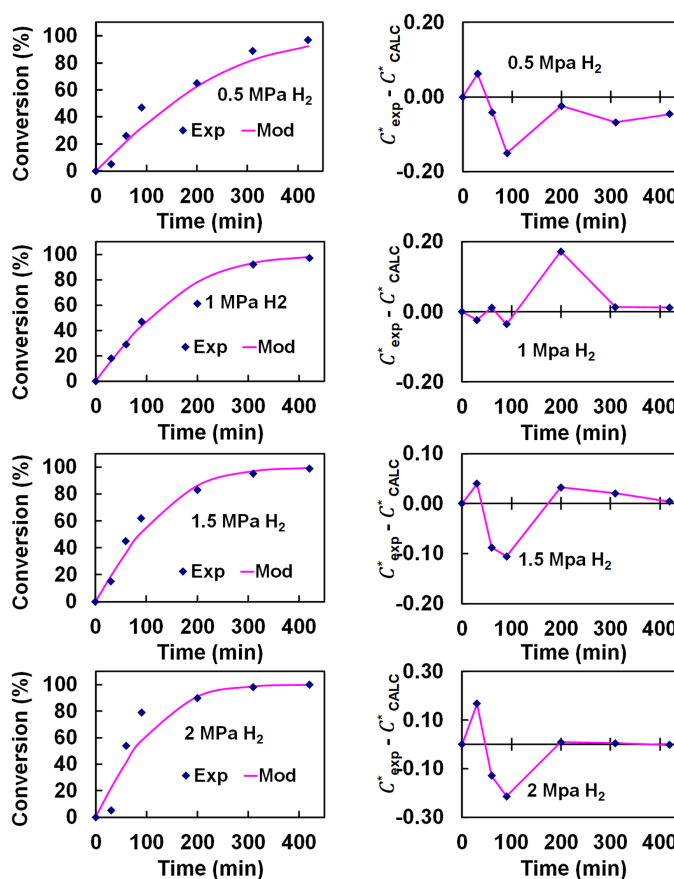


Figure 7. (Left) Aqueous phase hydrogenation (APH) of glucose with Ru (3%)/C. In symbols, experimental results and in solid lines the results using model 3a. (Right) Evolution of residuals. [$T = 363 \text{ K}$, $C_{\text{glu}}^0 = 0.1 \text{ M}$; $V_{\text{H}_2\text{O}} = 50 \text{ ml}$].

And the model 3a was adjusted with the data obtained for 343 - 383 K. The results are shown in **Table 4**, while the fit obtained for the different temperatures evaluated can be observed in **Figure 8**.

Table 4. Modeling results using all experiments and including the temperature dependency.

Parameter	Model 3a
k_0	3.71×10^1
E_a (kJ/mol)	8.69×10^3
ΔH_A (J/mol)	8.89×10^3
ΔS_A (J/(mol K))	6.04×10^1
ΔH_B (J/mol)	3.22×10^4
ΔS_B (J/(mol K))	7.54×10^1
ΔH_C (J/mol)	-3.04×10^4
ΔS_C (J/(mol K))	-5.18×10^1

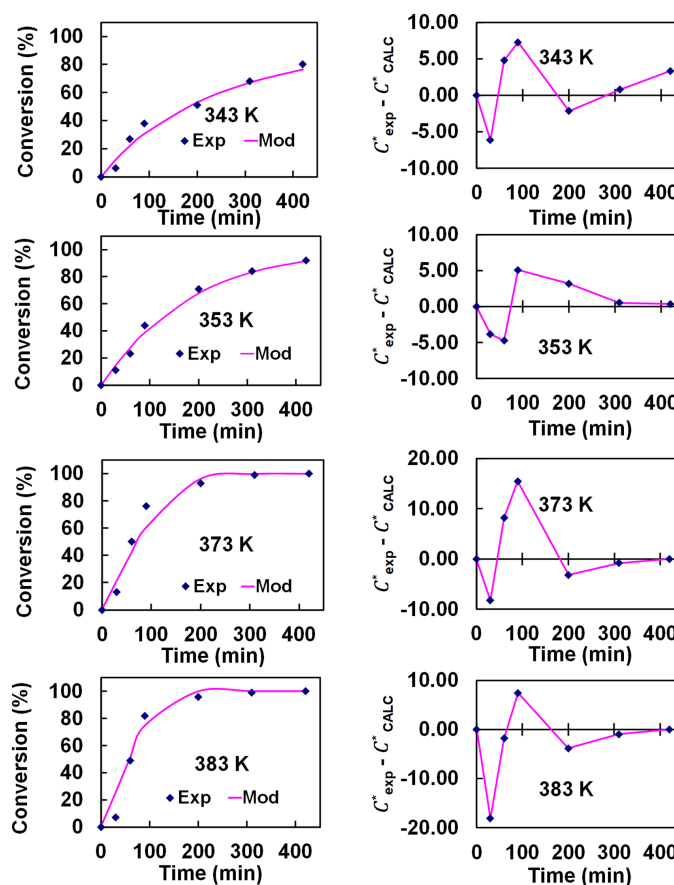


Figure 8. (left) Aqueous phase hydrogenation (APH) of glucose with Ru (3%)/C at different temperatures. In symbols, experimental results and in solid lines the results using model 3a. (Right) Evolution of residuals. [$p_{H_2} = 1.25$ MPa, $W_{CAT} = 250$ mg, $C^0_{glu} = 0.1$ M; $V_{H_2O} = 50$ ml].

The D-glucose adsorption enthalpy H_A presents a positive value. This is indicating that the adsorption constant of D-glucose increases with temperature. This is not thermodynamically consistent with adsorption phenomena. However, this behavior has been described by other authors in terms of the mechanism of D-glucose adsorption [24].

From the kinetic studies carried out, and considering the reaction mechanism proposed by model 3a, **Figure 9** represents a surface of ruthenium atoms supported on carbon on which hydrogen is adsorbed dissociatively and glucose does so through its hemiacetal group, leading to the formation of sorbitol, following the elementary steps described from (i) to (iv).

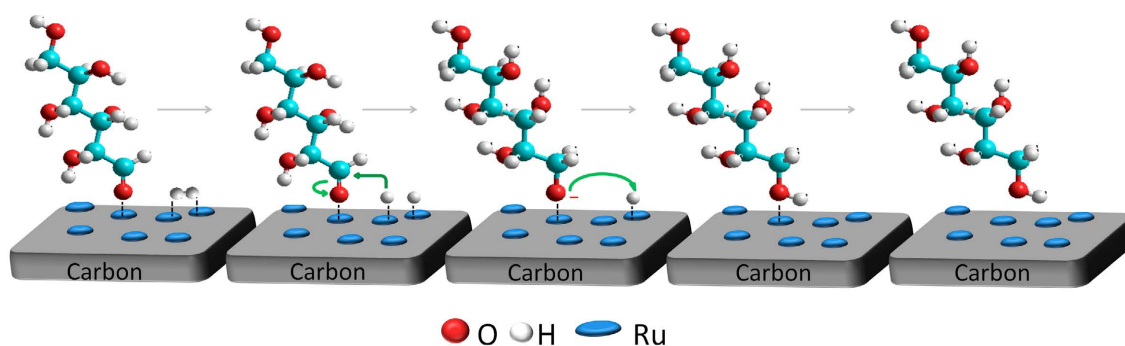


Figure 9. Elementary steps of the chemical reaction for proposed model 3a to the hydrogenation of glucose on Ru (3%)/C.

4. Conclusions

The 3 wt% Ru/C catalyst studied was highly selective towards sorbitol under the conditions tested (363 K and 1.25 MPa). These experimental conditions are milder than the ones generally reported for the APH reaction.

The kinetic study of D-glucose hydrogenation was carried out. The experimental data could be interpreted through LHHW heterogeneous models. The best fit was obtained when the competitive adsorption of both glucose and hydrogen was considered. Hydrogen is dissociative adsorbed and the rate-limiting step is the surface chemical reaction.

Acknowledgements

The authors would like to acknowledge the following institutions of Argentina for the financial support, UNNOBA (project SIB 2022, Exp. 1664/2022), CONICET (project PIP 0134/2021) and ANPCyT FONCyT (PICT 2019/1962).

Conflicts of Interest

The authors declare no conflicts of interest regarding the publication of this paper.

References

- [1] Li, N., Tompsett, G.A., Zhang, T., Shi, J., Wyman, C.E. and Huber, G.W. (2011)

- Renewable Gasoline from Aqueous Phase Hydrodeoxygenation of Aqueous Sugar Solutions Prepared by Hydrolysis of Maple Wood. *Green Chemistry*, **13**, 91-101. <https://doi.org/10.1039/C0GC00501K>
- [2] Negahdar, L., Delidovich, I. and Palkovits, R. (2016) Aqueous-Phase Hydrolysis of Cellulose and Hemicelluloses over Molecular Acidic Catalysts: Insights into the Kinetics and Reaction Mechanism. *Applied Catalysis B: Environmental*, **184**, 285-298. <https://doi.org/10.1016/j.apcatb.2015.11.039>
- [3] Climent, M.J., Corma, A. and Iborra, S. (2014) Conversion of Biomass Platform Molecules into Fuel Additives and Liquid Hydrocarbon Fuels. *Green Chemistry*, **16**, 516-547. <https://doi.org/10.1039/c3gc41492b>
- [4] Werpy, T. and Petersen, G. (2004) Top Value Added Chemicals from Biomass: Volume I—Results of Screening for Potential Candidates from Sugars and Synthesis Gas. <https://doi.org/10.2172/15008859>
- [5] Vilcocq, L., Cabiac, A., Espedel, C., Guillon, E. and Duprez, D. (2013) Transformation of Sorbitol to Biofuels by Heterogeneous Catalysis: Chemical and Industrial Considerations. *Oil & Gas Science and Technology*, **68**, 841-860. <https://doi.org/10.2516/ogst/2012073>
- [6] Zhang, X., Durndell, L.J., Isaacs, M.A., Parlett, C.M.A., Lee, A.F. and Wilson, K. (2016) Platinum-Catalyzed Aqueous-Phase Hydrogenation of d-Glucose to d-Sorbitol. *ACS Catalysis*, **6**, 7409-7417. <https://doi.org/10.1021/acscatal.6b02369>
- [7] Zhang, J., Lin, L., Zhang, J. and Shi, J. (2011) Efficient Conversion of D-Glucose into D-Sorbitol over MCM-41 Supported Ru Catalyst Prepared by a Formaldehyde Reduction Process. *Carbohydrate Research*, **346**, 1327-1332. <https://doi.org/10.1016/j.carres.2011.04.037>
- [8] Hoffer, B.W., Crezee, E., Mooijmana, P.R.M., van Langeveld, A.D., Kapteijn, F. and Moulijn, J.A. (2003) Carbon Supported Ru Catalysts as Promising Alternative for Raney-Type Ni in the Selective Hydrogenation of d-Glucose. *Catalysis Today*, **79-80**, 35-41. [https://doi.org/10.1016/S0920-5861\(03\)00040-3](https://doi.org/10.1016/S0920-5861(03)00040-3)
- [9] Gallezot, P., Cerino, P.J., Blanc, B., Fleche, G. and Fuytes, P. (1994) Glucose Hydrogenation on Promoted Raney-Nickel Catalysts. *Journal of Catalysis*, **146**, 93-102. [https://doi.org/10.1016/0021-9517\(94\)90012-4](https://doi.org/10.1016/0021-9517(94)90012-4)
- [10] Arena, B.J. (1992) Deactivation of Ruthenium Catalysts in Continuous Glucose Hydrogenation. *Applied Catalysis A: General*, **87**, 219-229. [https://doi.org/10.1016/0926-860X\(92\)80057-J](https://doi.org/10.1016/0926-860X(92)80057-J)
- [11] Delidovich, I. and Palkovits, R. (2016) Catalytic Isomerization of Biomass-Derived Aldoses: A Review. *ChemSusChem*, **9**, 547-561. <https://doi.org/10.1002/cssc.201501577>
- [12] Zhang, J., Li, J. and Lin, L. (2014) Dehydration of Sugar Mixture to HMF and Furfural over $\text{SO}_4^{2-}/\text{ZrO}_2\text{-TiO}_2$ Catalyst. *BioResources*, **9**, 4194-4204. <https://doi.org/10.15376/biores.9.3.4194-4204>
- [13] Banu, M., Sivasanker, S., Sankaranarayanan, T.M. and Venuvanalingam, P. (2011) Hydrogenolysis of Sorbitol over Ni and Pt Loaded on NaY. *Catalysis Communications*, **12**, 673-677. <https://doi.org/10.1016/j.catcom.2010.12.026>
- [14] Van Gorp, K., Boerman, E., Cavenaghi, C.V. and Berben, P.H. (1999) Catalytic Hydrogenation of Fine Chemicals: Sorbitol Production. *Catalysis Today*, **52**, 349-361. [https://doi.org/10.1016/S0920-5861\(99\)00087-5](https://doi.org/10.1016/S0920-5861(99)00087-5)
- [15] Hoffer, B.W., Crezee, E., Devred, F., Mooijman, P.R.M., Sloof, W.G., Kooyman, P.J., van Langeveld, A.D., Kaptejn, F. and Moulijn, J.A. (2003) The Role of the Active Phase of Raney-Type Ni Catalysts in the Selective Hydrogenation of d-Glucose to

- d-Sorbitol. *Applied Catalysis A: General*, **253**, 437-452.
[https://doi.org/10.1016/S0926-860X\(03\)00553-2](https://doi.org/10.1016/S0926-860X(03)00553-2)
- [16] Kusserow, B., Schimpf, S. and Claus, P. (2003) Hydrogenation of Glucose to Sorbitol over Nickel and Ruthenium Catalysts. *Advanced Synthesis & Catalysis*, **345**, 289-299.
<https://doi.org/10.1002/adsc.200390024>
- [17] Ahmed, M.J. and Hameed, B.H. (2019) Hydrogenation of Glucose and Fructose into Hexitols over Heterogeneous Catalysts: A Review. *Journal of the Taiwan Institute of Chemical Engineers*, **96**, 341-352. <https://doi.org/10.1016/j.jtice.2018.11.028>
- [18] Musci, J.J., Merlo, A.B. and Casella, M.L. (2017) Aqueous Phase Hydrogenation of Furfural Using Carbon-Supported Ru and RuSn Catalysts. *Catalysis Today*, **296**, 43-50.
<https://doi.org/10.1016/j.cattod.2017.04.063>
- [19] Bailón-García, E., Carrasco-Marín, F., Pérez-Cadenas, A.F. and Maldonado-Hodar, F.J. (2016) Selective Hydrogenation of Citral by Noble Metals Supported on Carbon Xerogels: Catalytic Performance and Stability. *Applied Catalysis A: General*, **512**, 63-73. <https://doi.org/10.1016/j.apcata.2015.12.017>
- [20] Meille, V., Pestre, N., Fongarland, P. and de Bellefon, C. (2004) Gas/Liquid Mass Transfer in Small Laboratory Batch Reactors: Comparison of Methods. *Industrial & Engineering Chemistry Research*, **43**, 924-927. <https://doi.org/10.1021/ie030569j>
- [21] Weisz, P.B. and Hicks, J.S. (1962) The Behaviour of Porous Catalyst Particles in View of Internal Mass and Heat Diffusion Effects. *Chemical Engineering Science*, **17**, 265-275. [https://doi.org/10.1016/0009-2509\(62\)85005-2](https://doi.org/10.1016/0009-2509(62)85005-2)
- [22] Weisz, P.B. and Prater, C.D. (1954) Interpretation of Measurements in Experimental Catalysis. *Advances in Catalysis*, **6**, 143-196.
[https://doi.org/10.1016/S0360-0564\(08\)60390-9](https://doi.org/10.1016/S0360-0564(08)60390-9)
- [23] Mishra, D.K., Dabbawala, A.A., Park, J.J., Jhung, S.H. and Hwang, J. (2014) Selective Hydrogenation of d-Glucose to d-Sorbitol over HY Zeolite Supported Ruthenium Nanoparticles Catalysts. *Catalysis Today*, **232**, 99-107.
<https://doi.org/10.1016/j.cattod.2013.10.018>
- [24] Crezee, E.B., Hoffer, B.W., Berger, R.J., Makkee, M., Kapteijn, F. and Moulijn, J.A. (2003) Three-Phase Hydrogenation of d-Glucose over a Carbon Supported Ruthenium Catalyst—Mass Transfer and Kinetics. *Applied Catalysis A: General*, **251**, 1-17.
[https://doi.org/10.1016/S0926-860X\(03\)00587-8](https://doi.org/10.1016/S0926-860X(03)00587-8)
- [25] Li, H., Chu, D., Liu, J., Qiao, M., Dai, W. and Li, H. (2008) A Novel Ruthenium-Phosphorus Amorphous Alloy Catalyst for Maltose Hydrogenation to Maltitol. *Advanced Synthesis & Catalysis*, **350**, 829-836.
<https://doi.org/10.1002/adsc.200700606>
- [26] Tukac, V. (1997) Glucose Hydrogenation in a Trickle-Bed Reactor. *Collection of Czechoslovak Chemical Communications*, **62**, 1423-1428.
<https://doi.org/10.1135/cccc19971423>
- [27] Guo, H., Li, H., Zhu, J., Ye, W., Qiao, M. and Dai, W. (2003) Liquid Phase Glucose Hydrogenation to d-Glucitol over an Ultrafine Ru-B Amorphous Alloy Catalyst. *Journal of Molecular Catalysis A: Chemical*, **200**, 213-221.
[https://doi.org/10.1016/S1381-1169\(03\)00008-6](https://doi.org/10.1016/S1381-1169(03)00008-6)